

000 SILVER STEPSIZE FOR FASTER ZEROTH-ORDER OPTI- 001 002 003 004 005 006 007 008 009 010 011 012 013 014 015 016 017 018 019 020 021 022 023 024 025 026 027 028 029 030 031 032 033 034 035 036 037 038 039 040 041 042 043 044 045 046 047 048 049 050 051 052 053 SILVER STEPSIZE FOR FASTER ZEROTH-ORDER OPTI- MIZATION

Anonymous authors

Paper under double-blind review

ABSTRACT

We study gradient-free minimization of smooth convex functions via *Silver stepsizes*, a non-monotone 2-adic schedule that accelerates gradient descent, composed with two-point zeroth-order (ZO) estimators on a smoothed objective. We show that the *multi-step Lyapunov (Silver) analysis* carries over when exact gradients are replaced by *conditionally unbiased* two-point estimators, with a stochastic tax that reduces to a *quadratic variance* term. We control this term under a fixed query budget by an *orthogonal-on-spikes* batching policy $B_t \propto \alpha_t$, which is *budget-optimal*. Empirically, we validate our approach on numerical quadratics across different conditioning regimes and *MeZO*-style forward-only fine-tuning of RoBERTa-large on GLUE tasks (SST-2, RTE), ZO-SILVER reduces evaluation loss faster than tuned constant-LR MeZO under the same query budget.

1 INTRODUCTION

Zeroth-order (ZO, derivative-free) optimization addresses the common setting where we can query function values but cannot reliably obtain gradients: the model is a black box, gradients are prohibitively expensive or noisy, or we wish to optimize through a non-differentiable system (e.g., simulators, private APIs). This regime occurs across machine learning and scientific computing: hyperparameter and architecture tuning, black-box adversarial attacks, policy search and evolution strategies in RL, and large-model fine-tuning under tight memory budgets (Larson et al., 2019; Flaxman et al., 2005; Duchi et al., 2015; Shamir, 2017; Salimans et al., 2017; Malladi et al., 2023a).

Families of ZO estimators. Modern ZO methods approximate gradients from function values using structured perturbations. (i) *One-point bandit smoothing* forms an unbiased estimator of the gradient of a smoothed objective from a single evaluation (Flaxman et al., 2005). (ii) *Two-point estimators*—our focus—use symmetric differences $f(x + \mu u) - f(x - \mu u)$ along a random direction u , achieving strictly better variance/rates and minimax-optimal guarantees for smooth convex objectives (Duchi et al., 2015; Shamir, 2017; Nesterov & Spokoiny, 2017). (iii) *Coordinate-wise finite differences* estimate partial derivatives one coordinate at a time (often $2d$ queries per gradient) and are widely used in black-box deep learning (e.g., ZOO attacks) (Chen et al., 2017). (iv) *SPSA* perturbs all coordinates simultaneously using Rademacher noise and recovers a two-evaluation gradient proxy with strong SA-style guarantees (Spall, 1992). (v) *Orthogonal batches* sample B mutually orthonormal directions (Stiefel manifold) per iteration; this reduces the estimator variance at fixed budget and unifies several schemes, including spherical smoothing and coordinate descent (Kozak et al., 2023; Feng & Wang, 2023).

Core bottlenecks in ZO. ZO estimators introduce a bias–variance tradeoff via the smoothing radius μ and sampling distribution. Even for smooth convex objectives, the best-known two-point schemes incur a statistical floor that scales with dimension under noisy queries; controlling the *variance accumulation* across iterations is the central algorithmic challenge (Duchi et al., 2015; Shamir, 2017; 2013; Jamieson et al., 2012).

An acceleration lever: stepsize hedging (Silver). Independently of estimator design, recent work shows that carefully structured *stepsizes* alone can accelerate plain gradient descent on smooth convex functions. The *Silver stepsize schedule* is a simple, explicit, fractal sequence with a 2-adic block structure. It admits a *multi-step Lyapunov certificate* (“Silver identity”) which gives a convergence

054 rate of $O(\varepsilon^{-\log_\rho 2}) = O(\varepsilon^{-0.7864})$ iterations for gradient descent, where $\rho = 1 + \sqrt{2}$ is the silver
 055 ratio (Altschuler & Parrilo, 2023a;b; 2024). Intuitively, the schedule interleaves small steps with
 056 periodic “spikes” whose algebraic cancellation accelerates net progress across blocks.
 057

058 **This work: composing Silver with two-point ZO on smoothed objectives.** We bring these strands
 059 together. We run the Silver schedule on a *smoothed* objective $h = f_\mu/L$ (blockwise-constant μ),
 060 and replace exact gradients by unbiased *symmetric two-point* estimators for ∇f_μ along *orthonormal*
 061 batches of directions. The Silver identity’s linear noise terms cancel in expectation, so the entire
 062 stochastic tax collapses to an explicit *quadratic variance term*, which we control by aligning batch
 063 size with the stepsize spikes ($B_t \propto \alpha_t$, capped at d). This *orthogonal-on-spikes* policy concentrates
 064 averaging where it matters most while keeping the total query budget fixed.
 065

066 **Motivation** Two-point estimators are unbiased for ∇f_μ (not ∇f), making the smoothed problem
 067 f_μ the right analytical object. The Silver identity is robust to *conditionally unbiased* inexact gradients
 068 and only pays the quadratic term from the terminal square in the certificate—precisely what batching
 069 and blockwise μ can control. Orthogonal directions improve constants without complicating the
 070 analysis or the memory footprint (Kozak et al., 2023; Feng & Wang, 2023).
 071

We make the following contributions in this work.

- 072 • Silver-on-smoothing with two-point ZO: We adapt the Silver multi-step analysis to $h =$
 073 f_μ/L with symmetric two-point estimators, showing the identity carries over with a single
 074 *variance aggregation* term $\sum_t \alpha_t^2 \mathbb{E}\|\zeta_t\|^2$ (no linear noise term).
- 075 • Variance control via orthogonal-on-spikes batching: Under a fixed query budget per block,
 076 we prove that allocating batch sizes proportional to the Silver steps ($B_t \propto \alpha_t$, capped at
 077 d) optimally controls $\sum_t \alpha_t^2/B_t$ (Cauchy–Schwarz tightness), and we instantiate this with
 078 Stiefel sampling.
- 079 • High-probability bounds via Freedman: We give a simple high-probability translation of
 080 the Silver identity with martingale differences, giving dimension-aware tails in terms of the
 081 predictable quadratic variation.
- 082 • Practical ZO for LLM fine-tuning: We apply the method to MeZO-style forward-only full-
 083 parameter fine-tuning and discuss practical details (direction orthogonalization, clipping,
 084 memory footprint.) (Malladi et al., 2023a; Hu et al., 2021; Dettmers et al., 2023).

085 **Organization.** Section 3.1 states the formal setup and notation; Section 3.2 summarizes the Silver
 086 schedule and the specific properties we use. Section 4 develops the inexact-gradient Silver identity
 087 for two-point ZO on f_μ and the variance control via orthogonal-on-spikes batching. Experiments
 088 appear in Section 5.
 089

090 2 RELATED WORK 091

092 **Derivative-free / zeroth-order optimization.** Classical DFO covers direct-search, model-based
 093 trust-region, and interpolation methods; recent surveys unify these with randomized finite-difference
 094 estimators used in ML (Larson et al., 2019). For convex ZO with random directions, one-point
 095 bandit smoothing dates to Flaxman et al. (2005). Two-point estimators achieve optimal rates in
 096 smooth/stochastic and adversarial settings (Duchi et al., 2015; Shamir, 2017). Nesterov & Spokoiny
 097 (2017) give a self-contained analysis with explicit smoothing constants. Building on this line of work,
 098 MeZO (Malladi et al., 2023a) brings two-point, forward-only ZO into LLM fine-tuning, showing that
 099 competitive adaptation is possible with inference-level memory (no backprop activations). In this
 100 work, we analyze with uniform sphere sampling for slightly tighter dimension-dependent estimation
 101 variance at high dimension.

102 **Estimator families and variance reduction.** Coordinate-wise finite differences (up to $2d$
 103 queries/gradient) are common in black-box deep learning, e.g., ZOO (Chen et al., 2017). SPSA
 104 provides a two-evaluation coordinate-free estimator rooted in stochastic approximation (Spall, 1992).
 105 Sampling *orthogonal* directions (Stiefel manifold) reduces variance and unifies spherical and coordinate
 106 schemes (Kozak et al., 2023); refined bounds appear in Feng & Wang (2023). Variance-reduced
 107 ZO methods (e.g., ZO-SVRG/SPIDER-SZO) are complementary and can be combined with our
 108 blockwise policy (Ji et al., 2019; Fang et al., 2018).

108 Zeroth-order smoothing and two-point estimators. Ball/sphere and Gaussian smoothing with
 109 two-point estimators are classical; see Flaxman et al. (2005) (one-point bandit smoothing), Duchi
 110 et al. (2015); Shamir (2017) (two-point optimal rates), and Nesterov & Spokoiny (2017) (Gaussian
 111 smoothing with explicit moment and bias constants). We emphasize the uniform *ball/sphere* pair,
 112 which gives dimension-friendly bias constants and a clean gradient identity.

113 Stepsize hedging / Silver schedule. The Silver schedule is a simple explicit fractal stepsize sequence
 114 that accelerates plain gradient descent in both strongly convex and smooth convex regimes. The
 115 analysis hinges on a multi-step descent identity and 2-adic structure; see Altschuler & Parrilo
 116 (2023a;b; 2024) for the arXiv and final journal versions. The rate $T^{-\log_\rho 2}$ with $\rho = 1 + \sqrt{2}$ lies
 117 between classical $O(\varepsilon^{-1})$ and Nesterov's $O(\varepsilon^{-1/2})$.
 118

119 3 PRELIMINARIES

121 3.1 PROBLEM SETUP AND NOTATION

123 We minimize a convex L -smooth function $f : \mathbb{R}^d \rightarrow \mathbb{R}$ with minimizer x^* . We adopt the standard
 124 uniform-ball smoothing

$$125 \quad f_\mu(x) := \mathbb{E}_{v \sim \text{Unif}(\mathbb{B}^d)} f(x + \mu v), \quad h(x) := f_\mu(x)/L,$$

127 so that h is 1-smooth and convex. We use the symmetric two-point estimator because it enjoys sharper
 128 variance/rate guarantees in smooth convex problems (Duchi et al., 2015; Shamir, 2017; Nesterov &
 129 Spokoiny, 2017).

130 **131 Uniform-ball smoothing and the sphere gradient identity.** Let $v \sim \text{Unif}(\mathbb{B}^d)$ and $u \sim$
 132 $\text{Unif}(\mathbb{S}^{d-1})$, and define $f_\mu(x) := \mathbb{E}_v f(x + \mu v)$. Then f_μ is convex and L -smooth and

$$133 \quad \nabla f_\mu(x) = \frac{d}{\mu} \mathbb{E}_u [f(x + \mu u) u]. \quad (1)$$

135 And,

$$136 \quad |f_\mu(x) - f(x)| \leq \frac{L}{2} \mu^2 \mathbb{E} \|v\|^2 = \frac{L}{2} \mu^2 \cdot \frac{d}{d+2}.$$

138 Moreover (proofs in the appendix),

$$139 \quad \|\nabla f_\mu(x) - \nabla f(x)\| \leq \frac{L}{2} d \mu. \quad (2)$$

141 For comparison, under *Gaussian* smoothing, $\|\nabla f_\mu(x) - \nabla f(x)\| \leq \frac{L}{2} (d+3)^{3/2} \mu$ (Nesterov &
 142 Spokoiny, 2017, Lemma 3).

143 *Remark 3.1* (Default smoothing and unbiasedness). Throughout we define $f_\mu(x) = \mathbb{E}_{v \sim \text{Unif}(\mathbb{B}^d)} f(x +
 144 \mu v)$. For this choice,

$$145 \quad \nabla f_\mu(x) = \frac{d}{\mu} \mathbb{E}_{u \sim \text{Unif}(\mathbb{S}^{d-1})} [f(x + \mu u) u],$$

147 so both the one-point $\frac{d}{\mu} f(x + \mu u) u$ and the symmetric two-point $\frac{d}{2\mu} (f(x + \mu u) - f(x - \mu u)) u$
 148 estimators are *unbiased* for $\nabla f_\mu(x)$. This identity goes back to the divergence-theorem proof used in
 149 bandit smoothing (e.g., Flaxman et al. (2005)).¹
 150

151 **Iteration, stepsizes, and batching.** We run a Silver block of length $N = 2^k - 1$ with stepsizes
 152 $\{\alpha_t\}_{t=0}^{N-1}$ (Section 3.2), update

$$154 \quad x_{t+1} = x_t - \frac{\alpha_t}{L} \widehat{g}_t, \quad \widehat{g}_t = \frac{d}{2\mu B_t} \sum_{i=1}^{B_t} (f(x_t + \mu v_{t,i}) - f(x_t - \mu v_{t,i})) v_{t,i},$$

156 and use *orthogonal-on-spikes* batching $B_t = \min\{d, \lceil c_B \alpha_t \rceil\}$ with $V_t = [v_{t,1}, \dots, v_{t,B_t}] \in$
 157 $\text{St}(d, B_t)$ drawn via thin QR of a Gaussian matrix (Haar on the Stiefel manifold). Each step
 158 costs $2B_t$ function queries. Unless stated otherwise, we assume access to exact function values or
 159 conditionally zero-mean value noise so that $\mathbb{E}[\widehat{g}_t | \mathcal{F}_{t-1}] = \nabla f_\mu(x_t)$ with \mathcal{F}_{t-1} the natural filtration
 160 up to the start of iteration t (so x_t, α_t are \mathcal{F}_{t-1} -measurable).
 161

¹We work with the *ball* definition of f_μ for tighter bias; we only use the *sphere* for the estimator.

162 3.2 SILVER STEPSIZES PRIMER
163164 Let $\rho := 1 + \sqrt{2}$ and let $v(i)$ be the 2-adic valuation of $i \in \mathbb{N}$. We use the explicit schedule
165

166
$$\alpha_i = 1 + \rho^{v(i)-1}, \quad i = 1, 2, \dots$$

167 (optionally scaled and/or clipped in practice). This closed form matches the recursive construction
168 and gives a fractal 2-adic block structure.(Altschuler & Parrilo, 2023a;b; 2024)

169 For a block of length $N = 2^k - 1$ and a 1-smooth convex objective h , Altschuler & Parrilo (2023b)
170 establish a multi-step Lyapunov identity which implies

171
$$h(x_N) - h^* \leq r_k \|x_0 - x^*\|^2,$$

172 with explicit

173
$$r_k := \frac{1}{1 + \sqrt{4\rho^{2k} - 3}} \leq \frac{1}{2\rho^{\log_2 n}} = \frac{1}{2n^{\log_2 \rho}} = O(n^{-1.2716})$$

174

175 for $\rho = 1 + \sqrt{2}$ (the silver ratio). This rate improves upon the classical Gradient Descent convergence
176 of $O(1/n)$, positioning itself as an intermediary between this baseline and the accelerated convergence
177 rate $O(1/n^2)$ of Nesterov's method, which is known to be optimal for first-order smooth convex
178 optimization (Nesterov, 1983; Nemirovsky & Yudin, 1983). This improvement is achieved without
179 modifying the algorithmic structure or introducing momentum terms, only through an appropriate
180 choice of step sizes. Consequently, after $N = \Theta(2^k)$ steps, gradient descent with Silver stepsizes
181 reaches error ε in $O(\varepsilon^{-\log_\rho 2}) = O(\varepsilon^{-0.7864})$ iterations, strictly improving upon the classical $O(1/\varepsilon)$
182 rate for smooth convex objectives (Altschuler & Parrilo, 2023a;b; 2024). In our analysis we apply
183 this identity to $h = f_\mu/L$ and rely only on:184 1. the block guarantee $h(x_N) - h^* \leq r_k \|x_0 - x^*\|^2$;
185 2. the sum-of-steps property $\sum_{t=0}^{N-1} \alpha_t = \Theta(\rho^k)$;
186 3. robustness to *conditionally unbiased* inexact gradients, which adds exactly $\sum_t \alpha_t^2 \mathbb{E}\|\zeta_t\|^2$ to the
187 RHS (no linear noise term).
188189 4 ZO-SILVER: ALGORITHM AND THEORETICAL ANALYSIS
190191 ROADMAP OF THIS SECTION
192193 We state the blockwise guarantees first: (i) an expectation-level *one-block* bound under two-point ZO
194 on the smoothed objective with Silver steps; (ii) a *budget-aligned* specialization under orthogonal-on-
195 spikes batching; (iii) a *multi-block* (restart) bound; and (iv) a *high-probability* version via Freedman.
196 We then present the algorithm (with Stiefel sampling) and the minimal ingredients (unbiasedness,
197 second moment, inexact-Silver identity, and the variance-optimal batching proposition).
198199 4.1 ASSUMPTIONS AND ORACLE MODEL
200201 **Problem class and oracle** $f : \mathbb{R}^d \rightarrow \mathbb{R}$ is convex and L -smooth. We query a value oracle that
202 returns either exact $f(x)$ or $f(x) + \xi$ with conditionally zero-mean noise ($\mathbb{E}[\xi | x] = 0$) and finite
203 variance. We adopt uniform-ball smoothing $f_\mu(x) = \mathbb{E}_{v \sim \text{Unif}(\mathbb{B}^d)} f(x + \mu v)$ and define $h := f_\mu/L$,
204 so that h is 1-smooth and convex. Within each Silver block, μ is fixed. At iteration t , we form the
205 symmetric two-point estimator with B_t unit directions $V_t = [v_{t,1}, \dots, v_{t,B_t}] \in \text{St}(d, B_t)$ sampled
206 independently of the past and use the same batch for $\pm\mu$ queries.
207208 4.2 INGREDIENTS (UNBIASEDNESS, SECOND MOMENT, INEXACT SILVER, BATCHING)
209210 **Lemma 4.1** (Second moment: uniform sphere, symmetric two-point). *Let $f \in C_L^{1,1}$, $u \sim$
211 $\text{Unif}(\mathbb{S}^{d-1})$, and $\hat{g}(x; \mu, u) = \frac{d}{2\mu} (f(x + \mu u) - f(x - \mu u))u$. Then*

212
$$\mathbb{E}\|\hat{g}(x; \mu, u) - \nabla f_\mu(x)\|^2 \leq C_{\text{sig}} d \|\nabla f(x)\|^2 + C_{\text{curv}} d^2 L^2 \mu^2,$$

213

214 with $(C_{\text{sig}}, C_{\text{curv}}) = (2, \frac{1}{2})$. Averaging any $B \geq 1$ unit directions gives a $1/B$ reduction. Using
215 B orthonormal directions (Stiefel sampling) preserves the $1/B$ factor and improves constants in
practice (Kozak et al., 2023; Feng & Wang, 2023).

These constants are tight up to lower-order terms for two-point ZO under L -smoothness; see the elementary proof in the appendix and the companion derivation we follow. The proof is in the Appendix A.

Filtration and conditional unbiasedness. Let \mathcal{F}_{t-1} denote the σ -field generated by all randomness up to the *start* of iteration t (so x_t and α_t are \mathcal{F}_{t-1} -measurable). At iteration t , sample fresh directions V_t independently of \mathcal{F}_{t-1} (uniform on \mathbb{S}^{d-1} or Haar on $\text{St}(d, B_t)$), and evaluate f exactly (or with conditionally zero-mean noise) using the same batch for the $\pm\mu$ queries. For the symmetric two-point estimator we then have

$$\mathbb{E}[\hat{g}_t \mid \mathcal{F}_{t-1}] = \nabla f_\mu(x_t), \quad \zeta_t := \frac{1}{L}(\hat{g}_t - \nabla f_\mu(x_t)), \quad \mathbb{E}[\zeta_t \mid \mathcal{F}_{t-1}] = 0.$$

With predictable stepsizes (α_t) , define the predictable quadratic variation

$$V := \sum_{t=0}^{N-1} \alpha_t^2 \mathbb{E}[\zeta_t \zeta_t^\top \mid \mathcal{F}_{t-1}].$$

Lemma 4.2 (Martingale square identity). *Let $\{\zeta_t\}_{t=0}^{N-1}$ be a square-integrable vector MDS adapted to (\mathcal{F}_t) , so $\mathbb{E}[\zeta_t \mid \mathcal{F}_{t-1}] = 0$, and let $\{\alpha_t\}$ be deterministic (or merely \mathcal{F}_{t-1} -measurable). Then*

$$\mathbb{E} \left\| \sum_{t=0}^{N-1} \alpha_t \zeta_t \right\|^2 = \sum_{t=0}^{N-1} \alpha_t^2 \mathbb{E} \|\zeta_t\|^2.$$

Proof. Expand the square; for $s < t$, $\mathbb{E}\langle \zeta_s, \zeta_t \rangle = \mathbb{E}[\langle \zeta_s, \mathbb{E}[\zeta_t \mid \mathcal{F}_{t-1}] \rangle] = 0$, since ζ_s is \mathcal{F}_{t-1} -measurable. \square

4.3 MAIN RESULTS

Lemma 4.3 (Inexact Silver, expectation level). *Let $h = f_\mu/L$ (so h is 1-smooth and convex) and suppose $x_{t+1} = x_t - \alpha_t(\nabla h(x_t) + \zeta_t)$ with $\mathbb{E}[\zeta_t \mid \mathcal{F}_{t-1}] = 0$. For a Silver block $N = 2^k - 1$,*

$$\mathbb{E}[h(x_N) - h^*] \leq r_k \mathbb{E}\|x_0 - x^*\|^2 + \sum_{t=0}^{N-1} \alpha_t^2 \mathbb{E}\|\zeta_t\|^2.$$

Proof. See Appendix. \square

Variance-optimal batching under a query budget. We motivate the batching policy with the following variance-related observation.

Proposition 4.4 (Optimal allocation of directions under a query budget). *Fix nonnegative weights $\{\alpha_t\}_{t=0}^{N-1}$ and a budget $Q > 0$ of function queries per block. With symmetric two-point queries, $Q = 2 \sum_t B_t$. Then, for any $B_t > 0$,*

$$\sum_{t=0}^{N-1} \frac{\alpha_t^2}{B_t} \geq \frac{(\sum_{t=0}^{N-1} \alpha_t)^2}{\sum_{t=0}^{N-1} B_t} = \frac{2(\sum_t \alpha_t)^2}{Q},$$

with equality iff $B_t \propto \alpha_t$. In particular, the policy $B_t = \min\{d, \lceil c_B \alpha_t \rceil\}$ is (up to the cap and integrality) optimal for a given budget.

Proof. By Cauchy–Schwarz, $\left(\sum \frac{\alpha_t^2}{B_t}\right) (\sum B_t) \geq (\sum \alpha_t)^2$. Substitute $\sum B_t = Q/2$. \square

Theorem 4.5 (One block, expectation). *Assume $f : \mathbb{R}^d \rightarrow \mathbb{R}$ is convex and L -smooth, and fix a Silver block of length $N = 2^k - 1$ with steps $\{\alpha_t\}_{t=0}^{N-1}$. Let f_μ be the uniform-ball smoothing, $h = f_\mu/L$, and define the symmetric two-point estimator averaged over B_t unit directions (orthonormal columns $V_t \in \text{St}(d, B_t)$ drawn independently of \mathcal{F}_{t-1})*

$$\hat{g}_t = \frac{d}{2\mu B_t} \sum_{i=1}^{B_t} (f(x_t + \mu v_{t,i}) - f(x_t - \mu v_{t,i})) v_{t,i}, \quad x_{t+1} = x_t - \frac{\alpha_t}{L} \hat{g}_t.$$

270 *Then*

$$272 \quad \mathbb{E}[f(x_N) - f^*] \leq r_k L \mathbb{E}\|x_0 - x^*\|^2 + \sum_{t=0}^{N-1} \frac{\alpha_t^2}{B_t} \left(\frac{1}{2} d^2 L \mu^2 + \frac{2d}{L} \mathbb{E}\|\nabla f(x_t)\|^2 \right) + \frac{L}{2} \mu^2 \frac{d}{d+2}.$$

$$273$$

$$274$$

275 *In particular, if $\|x_t - x^*\| \leq R$, then $\|\nabla f(x_t)\| \leq LR$ and*

$$277 \quad \mathbb{E}[f(x_N) - f^*] \leq r_k L R^2 + \left(2d R^2 + \frac{1}{2} d^2 \mu^2 \right) \sum_{t=0}^{N-1} \frac{\alpha_t^2}{B_t} + L \mu^2 \frac{d}{d+2}.$$

$$278$$

$$279$$

280 *Proof sketch.* We apply the inexact-gradient Silver identity to $h = f_\mu/L$ with $\zeta_t = (\hat{g}_t - \nabla f_\mu(x_t))/L$
 281 (conditionally unbiased, so the identity has no linear noise term). Use the two-point second-moment
 282 bound plus averaging-by- B_t , then convert from h to f using the value-bias of f_μ . (see Appendix.) \square

$$283$$

284 **Budget-aligned specialization.** Let $B_t = \min\{d, \lceil c_B \alpha_t \rceil\}$ (orthogonal-on-spikes), and write
 285 $\alpha_{\max} = \max_t \alpha_t$. Then

286 **Proposition 4.6** (Variance aggregation under $B_t \propto \alpha_t$).

$$288 \quad \sum_{t=0}^{N-1} \frac{\alpha_t^2}{B_t} \leq \frac{1}{c_B} \sum_{t=0}^{N-1} \alpha_t + \frac{\alpha_{\max}}{d} \sum_{t: \alpha_t > d/c_B} \alpha_t.$$

$$289$$

$$290$$

291 *In particular, if $d \geq c_B \alpha_{\max}$ (cap inactive), then $\sum_t \alpha_t^2 / B_t = (1/c_B) \sum_t \alpha_t = \Theta(\rho^k / c_B)$.*292 **Corollary 4.7** (Per-block calibration of μ and c_B). *If $\frac{\rho^k}{c_B} \cdot \left(\frac{1}{2} d^2 L \mu^2 + 2d LR^2 \right) \leq \varepsilon r_k LR^2$, then*

$$295 \quad \mathbb{E}[f(x_N) - f^*] \leq (1 + \varepsilon) r_k LR^2 + \frac{L}{2} \mu^2 \frac{d}{d+2}.$$

$$296$$

297 *A sufficient choice is $c_B \geq \frac{2d \rho^k}{\varepsilon r_k}$ and $\mu^2 \leq \frac{2\varepsilon r_k}{d^2} \frac{R^2}{\rho^k}$.*299 **Theorem 4.8** (Multi-block restarts). *Run blocks $j = 1, \dots, J$ with lengths $N_j = 2^{k_j} - 1$ and radii
 300 μ_j (each fixed within the block), using $B_t = \min\{d, \lceil c_B \alpha_t \rceil\}$. If $\|x_t - x^*\| \leq R$ across the run, then*

$$302 \quad \mathbb{E}[f(x_{T_J}) - f^*] \leq LR^2 \sum_{j=1}^J r_{k_j} + \frac{1}{c_B} \sum_{j=1}^J \left(\frac{1}{2} d^2 L \mu_j^2 + 2d LR^2 \right) \rho^{k_j} + \frac{L}{2} \mu_J^2 \frac{d}{d+2}.$$

$$303$$

$$304$$

305 *Remark 4.9* (Empirical status of Silver in first-order GD). As far as we are aware, the original Silver
 306 papers and their support material emphasize theoretical certificates, and do not provide systematic
 307 first-order empirical benchmarks. Discussions on empirical observations and generalizations (e.g.,
 308 proximal/projected GD) are included, but a standardized FO benchmark suite on Silver vs. standard
 309 schedules has not yet emerged. See Altschuler & Parrilo (2023a;b; 2024); Parrilo (2024); Altschuler
 310 & Parrilo (2023c); Bok & Altschuler (2024).

311

4.4 ALGORITHM

312

 Algorithm 1 ZO-SILVER: block-constant smoothing + orthogonal-on-spikes batching

- 315 1: **Input:** block length $N = 2^k - 1$, radius $\mu > 0$, Silver steps $\{\alpha_t\}$, cap d , batching constant
 $c_B > 0$
- 316 2: **for** $t = 0, \dots, N - 1$ **do**
- 317 3: Stepsize $\eta_t = \alpha_t / L$; Batch $B_t = \min\{d, \lceil c_B \alpha_t \rceil\}$
- 318 4: Sample $V_t = [v_{t,1}, \dots, v_{t,B_t}] \in \text{St}(d, B_t)$ (orthonormal columns; e.g., thin QR of a Gaussian
 319 matrix)
- 320 5: $\hat{g}_t = \frac{d}{2\mu B_t} \sum_{i=1}^{B_t} (f(x_t + \mu v_{t,i}) - f(x_t - \mu v_{t,i})) v_{t,i}$
- 321 6: $x_{t+1} = x_t - \eta_t \hat{g}_t$

324 **Sampling orthonormal directions.** A simple implementation samples $G \in \mathbb{R}^{d \times B_t}$ with i.i.d.
 325 $\mathcal{N}(0, 1)$ entries and sets V_t to the Q factor of the thin QR decomposition $G = V_t R$, giving $V_t \in$
 326 $\text{St}(d, B_t)$ with Haar-distributed columns.
 327

328 **Corollary 4.10** (Per-block calibration of μ and batching). *Fix a block of length $N = 2^k - 1$ with*
 329 *$B_t = \min\{d, \lceil c_B \alpha_t \rceil\}$. Assume $\|\nabla f(x_t)\| \leq LR_t$ along the block (e.g., by projection or local*
 330 *boundedness). If we choose μ and c_B to satisfy $\frac{\rho^k}{c_B} \cdot \left(\frac{1}{2}d^2L\mu^2 + 2dLR_t^2\right) \leq \varepsilon \cdot r_k LR_t^2$, then the*
 331 *block guarantee becomes*
 332

$$334 \quad \mathbb{E}[f(x_N) - f^*] \leq (1 + \varepsilon) r_k LR_t^2 + \frac{L}{2} \mu^2 \frac{d}{d+2}.$$

335 *Equivalently, one sufficient choice is $c_B \geq \frac{2d\rho^k}{\varepsilon r_k}$ and $\mu^2 \leq \frac{2\varepsilon r_k}{d^2} \cdot \frac{R_t^2}{\rho^k}$.*
 336

337 **Remark 4.11.** In addition to the expectation-level bounds presented, we present high-probability
 338 results (see Appendix), to further justify our design choices, in particular the batching policy adopted.
 339

340 5 EXPERIMENTS

341 This section evaluates on two settings: (i) controlled, strongly-convex *quadratics* varying condition
 342 number and dimension, and (ii) *forward-only* MeZO-style fine-tuning on GLUE tasks (SST-2,
 343 RTE) using RoBERTa-large. Across both, we enforce budget-fairness (same number of function
 344 evaluations).

345 **Two-point ZO and budget matching.** Each iteration uses the symmetric two-point estimator
 346 (Sec. 3.1); querying B_t directions costs $2B_t$ function calls. We report and *match* $Q = 2 \sum_t B_t$
 347 across methods. We keep smoothing μ *block-constant* and use the same μ across baselines to isolate
 348 scheduling effects.

349 We compare against a tuned **ZO-GD (constant LR)** baseline that uses the *same* two-point estimator,
 350 smoothing μ , and matched query budget.

351 We first start by a quadratic test case, across different conditionings and dimensions, we then evaluate
 352 on two GLUE classification tasks: *SST-2* (binary sentiment) and *RTE* (recognizing textual entailment).
 353 We adopt the MeZO forward-only two-point estimator and compare (i) constant learning rate baselines
 354 to (ii) ZO-SILVER with clipped Silver stepsizes. We match the per-step query budget across both
 355 methods (Silver uses the same base LR, and the constant-LR baseline is additionally matched to the
 356 running-average of the clipped Silver multipliers).

357 5.1 QUADRATIC SUITE: PLOTS ACROSS CONDITIONING AND DIMENSION

358 We minimize ridge-type quadratics with prescribed condition numbers $\kappa \in \{5, 20, 35, 50\}$ and
 359 dimensions $d \in \{200, 500, 1000\}$. Each panel shows *function value vs. iterations* on a log *y*-scale;
 360 per-step budgets are matched.

361 **Observation.** On easy instances, ZO-Silver closely tracks the tuned constant-LR baseline; spikes do
 362 not destabilize training and sometimes provide a slight late-phase edge. As d increases, the late-phase
 363 gap widens: ZO-Silver's non-monotone spikes consistently accelerate log-decay at matched budgets.
 364 In the ill-conditioned regime: ZO-Silver shows an advantage in later iterations, and reaches lower
 365 final values with the same number of queries.

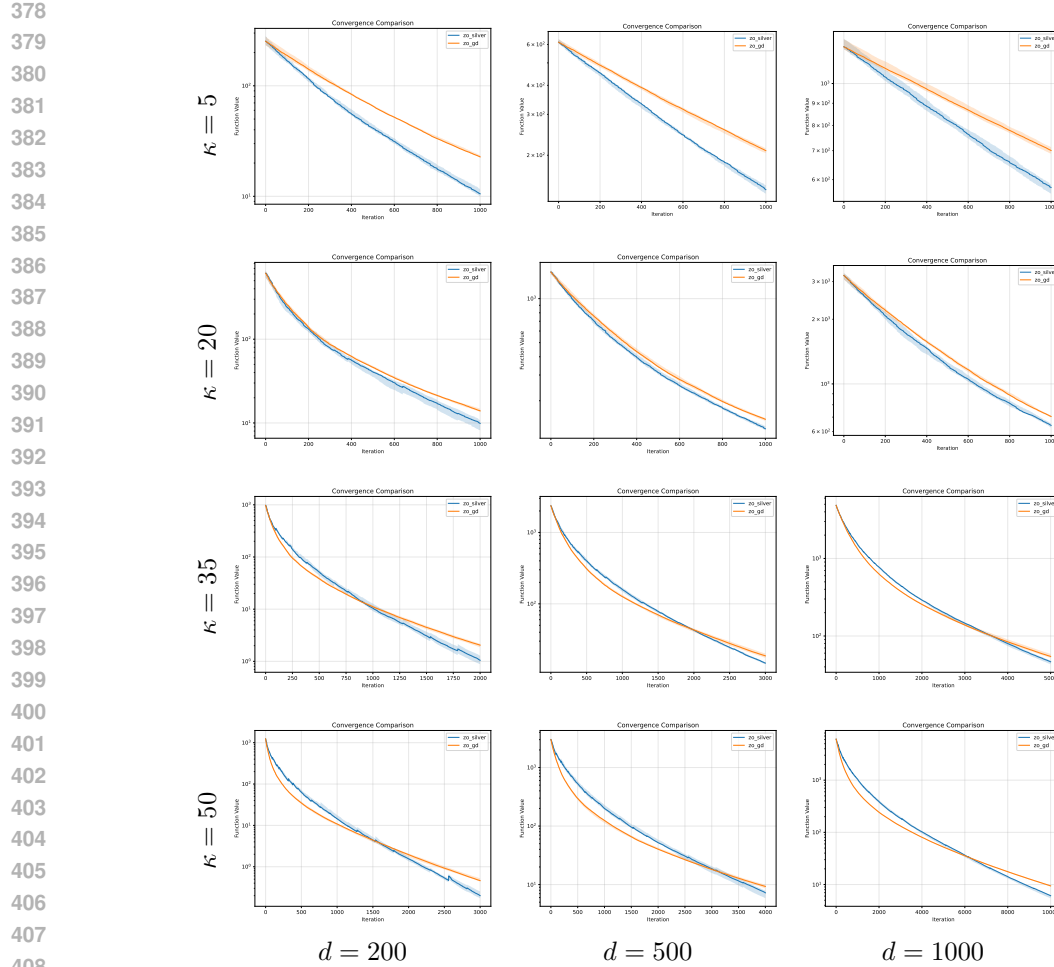


Figure 1: Quadratics, $\kappa = 5$: ZO-Silver vs. tuned constant-LR under matched query budgets. $\kappa = 20$: growing advantage of ZO-Silver with dimension. $\kappa = 35, 50$: ZO-Silver excels in later iterations under equal budgets.

Summary across different dimensions and condition regimes. ZO-Silver is *never worse* in well-conditioned cases and becomes increasingly *better* as conditioning (κ) and dimension (d) rise. We validate this observation in the second part of our empirical experiments on LLM-finetuning test cases, which are characterized by high conditioning and large dimension.

5.2 EXPERIMENTS ON ZEROTH-ORDER FINE-TUNING LLMs

We consider two GLUE classification tasks: *SST-2* (binary sentiment) and *RTE* (binary entailment). We fine-tune RoBERTa-large with two-point MeZO updates. For κ , we use a *clipped* schedule with max multiplier α_{\max} and match the *mean LR* to the constant-LR baseline to isolate scheduling effects.

PRELIMINARIES: MODEL, TASK, AND SETTING

Model. We fine-tune *RoBERTa-large*, a 24-layer masked-LM pretrain replica/extension of BERT with an improved training recipe and larger corpora; RoBERTa established strong results on GLUE and other benchmarks.² Liu et al. (2019)

²See Liu et al. (2019).

Benchmark. GLUE is a standard multi-task NLU benchmark; we focus on two classification tasks that are widely used in few-shot studies: *SST-2* (binary sentiment) and *RTE* (textual entailment).³ Wang et al. (2019); Socher et al. (2013); tfd

Tasks. *SST-2* consists of single-sentence movie-review snippets labeled *positive/negative* (Socher et al., 2013); *RTE* asks whether a hypothesis is entailed by a premise, derived from the PASCAL/TAC RTE challenges (Dagan et al., 2005; Bentivogli et al., 2009). Socher et al. (2013); tfd; Dagan et al. (2005); Bentivogli et al. (2009)

Few-shot protocol. We adopt the common $K=16$ few-shot split per task (prompted examples plus dev/test) and run full-parameter, forward-only optimization. This isolates the effect of stepsize scheduling in the constrained-sample regime (Wang et al., 2019). Wang et al. (2019)

Forward-only (MeZO). MeZO fine-tunes LMs using a two-point, forward-only zeroth-order estimator (two forward passes per update), achieving an inference-level memory footprint and supporting full-parameter or PEFT variants (Malladi et al., 2023b). Our runs keep the per-step forward-pass budget identical across schedulers. Malladi et al. (2023b)

447 SCHEDULERS AND FAIRNESS

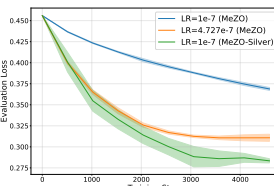
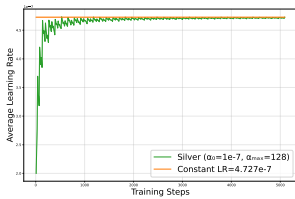
Clipped Silver vs. constant LR. We compare (i) MeZO with a constant learning rate and (ii) MeZO-SILVER, which uses Silver stepsizes with clipping $\alpha_t^{\text{clip}} = \min\{\alpha_t, \alpha_{\max}\}$. To attribute gains purely to *when* learning-rate mass is deployed, the constant-LR baseline is set to the *running-average* LR induced by the clipped Silver multipliers times the same base LR. If

$$J = \left\lfloor 1 + \log_{\rho}(\alpha_{\max} - 1) \right\rfloor, \quad \lim_{n \rightarrow \infty} \frac{1}{n} \sum_{t=0}^{n-1} \min\{\alpha_t, \alpha_{\max}\} = \left(\frac{\rho}{2}\right)^{J+1} + 2^{-(J+1)}(\alpha_{\max} - 1),$$

then with base LR 10^{-7} and $\alpha_{\max} = 128$, the matched constant LR is $\approx 4.727 \times 10^{-7}$.

Learning-rate schedule sanity check. Figure 2 plots the running-average learning rate induced by the clipped Silver schedule (base LR 10^{-7} ; clip $\alpha_{\max} = 128$) and the constant LR chosen to match that mean. This controls for mean-LR effects when comparing schedulers.

Setup: Few-shot $K=16$; **5,000 steps** with **evaluation every 500 steps**; logging every 10 steps; per-device train batch 64; per-device eval batch 4. All schedulers use the same two-point estimator, hence the same per-step forward-pass budget.



466
467
468
469
470
471
472
473
474
475
476
477
478
479
Figure 2: Clipped Silver schedule vs. constant LR baseline. We plot the running average learning rate induced by the Silver stepsizes with base learning rate $1e-7$ and clipping value 128.

480
481
482
483
484
485
Figure 3: Evaluation loss vs. training steps for RoBERTa-large fine-tuning on (a) SST-2 and (b) RTE. We compare standard MeZO with constant learning rates to MeZO-Silver using a clipped Silver schedule.

6 CONCLUSION

This work, with the theoretical analysis and subsequent experimental work presented shows non-monotone *Silver* stepsizes pair naturally with two-point zeroth-order (ZO) estimators when we

³GLUE: Wang et al. (2019). SST-2 originates from the Stanford Sentiment Treebank (Socher et al., 2013); GLUE’s RTE combines examples from RTE1–3 and RTE5.

486 optimize a smoothed objective. More broadly, our results provide the first step toward bringing
 487 stepsize hedging into the ZO regime: the Silver schedule, originally proved to accelerate plain gradient
 488 descent for smooth convex optimization, translates to the smoothed problem with conditionally
 489 unbiased ZO gradients, and preserves its deterministic multi-step progress up to standard ZO floors,
 490 compared with a constant stepsize scheme.

491 Empirically, we validated these claims in two complementary settings. On controlled, strongly-convex
 492 quadratics, is never worse than a carefully tuned constant-LR ZO baseline on well-conditioned
 493 instances, and it increasingly outperforms as the condition number and dimension grow, precisely
 494 where variance management matters most. In a forward-only fine-tuning regime (MeZO-style
 495 updates) on GLUE tasks (SST-2, RTE) with RoBERTa-large, clipped Silver steps combined with
 496 budget-aware batching give faster evaluation-loss decay and earlier stabilization than constant-LR
 497 under the *same* forward-pass budget.

498 **Limitations** Our analysis assumes convex, L -smooth objectives and focuses on two-point estimators
 499 with orthonormal direction batches; the LLM experiments could be further expanded to a more
 500 comprehensive benchmark. ZO methods as it is traditionally known can also incur higher query
 501 complexity than FO methods; throughput can become a bottleneck if the per-step budget is very
 502 small.
 503

504 **Outlook and Future Directions** Several directions look promising: (i) combining Silver with
 505 variance-reduced ZO estimators and adaptive batching; (ii) proximal and constrained variants (pro-
 506 jected/regularized objectives); (iii) task-aware smoothing schedules and spike-aware data reuse for
 507 forward-only fine-tuning; and (iv) extending the inexact Silver certificate beyond convexity (e.g.,
 508 PL or one-point weakly convex settings). We hope this work helps position *stepsize hedging* as
 509 a broadly useful knob in practical ZO optimization, especially in memory-constrained fine-tuning
 510 where forward-only updates are attractive.

511
 512
 513
 514
 515
 516
 517
 518
 519
 520
 521
 522
 523
 524
 525
 526
 527
 528
 529
 530
 531
 532
 533
 534
 535
 536
 537
 538
 539

540 REFERENCES

541
542 Glue in tensorflow datasets (rte configuration). <https://www.tensorflow.org/datasets/catalog/glue>. Accessed 2025-10-18.

543
544 Jason M. Altschuler and Pablo A. Parrilo. Acceleration by stepsize hedging i: Multi-step descent and
545 the silver stepsize schedule. *arXiv preprint*, 2023a. URL <https://arxiv.org/abs/2309.07879>.

546
547 Jason M. Altschuler and Pablo A. Parrilo. Acceleration by stepsize hedging ii: Silver stepsize
548 schedule for smooth convex optimization. *arXiv preprint*, 2023b. URL <https://arxiv.org/abs/2309.16530>.

549
550 Jason M. Altschuler and Pablo A. Parrilo. Support material for Acceleration by Stepsize Hedging.
551 <https://jasonaltschuler.github.io/AccelerationByStepsizeHedging/>,
552 2023c.

553
554 Jason M. Altschuler and Pablo A. Parrilo. Acceleration by stepsize hedging ii: Silver stepsize
555 schedule for smooth convex optimization. *Mathematical Programming*, 199:1179–1219, 2024.
556 doi: 10.1007/s10107-024-02164-2. URL <https://link.springer.com/article/10.1007/s10107-024-02164-2>. Final journal version.

557
558 Luisa Bentivogli, Ido Dagan, Danilo Giampiccolo, Bernardo Magnini, and Fabio Massimo Zanzotto.
559 The fifth PASCAL recognizing textual entailment challenge. In *Proceedings of the Text Analysis
560 Conference (TAC)*, Gaithersburg, MD, USA, 2009. NIST.

561
562 Jinho Bok and Jason M. Altschuler. Accelerating proximal gradient descent via silver step-
563 sizes. https://optimization-online.org/wp-content/uploads/2024/12/proxgd_stepsize_accel.pdf, 2024. arXiv:2412.05497.

564
565 Pin-Yu Chen, Huan Zhang, Yash Sharma, Jinfeng Yi, and Cho-Jui Hsieh. ZOO: Zeroth order
566 optimization based black-box attacks to deep neural networks. In *Proceedings of the 10th Workshop
567 on Artificial Intelligence and Security*, 2017.

568
569 Ido Dagan, Oren Glickman, and Bernardo Magnini. The PASCAL recognising textual entailment
570 challenge. In *Proceedings of the PASCAL Challenges Workshop on Recognising Textual Entailment*,
571 2005.

572
573 Tim Dettmers, Artidoro Pagnoni, Ari Holtzman, and Luke Zettlemoyer. Qlora: Efficient finetuning
574 of quantized llms. *NeurIPS*, 2023. URL <https://arxiv.org/abs/2305.14314>.

575
576 John C Duchi, Michael I Jordan, Martin J Wainwright, and Andre Wibisono. Optimal rates for
577 zero-order convex optimization: The power of two function evaluations. *IEEE Transactions on
578 Information Theory*, 61(5):2788–2806, 2015.

579
580 Cong Fang, Chris Junchi Li, Zhouchen Lin, and Tong Zhang. Spider: Near-optimal non-convex
581 optimization via stochastic path-integrated differential estimator. In *Advances in Neural In-
582 formation Processing Systems (NeurIPS)*, 2018. URL <https://proceedings.neurips.cc/paper/2018/file/ba9a56ce0a9bfa26e8ed9e10b2cc8f46-Paper.pdf>. ZO
583 variants discussed in follow-ups.

584
585 Yasong Feng and Tianyu Wang. Stochastic zeroth order gradient and hessian estimators: Variance
586 reduction and refined bias bounds. *Information and Inference: A Journal of the IMA*, 12(3):1514–
587 1545, 2023. doi: 10.1093/imaiai/iaad014. URL <https://academic.oup.com/imaiai/article/12/3/1514/7150743>.

588
589 Abraham D. Flaxman, Adam Tauman Kalai, and H. Brendan McMahan. Online convex optimization
590 in the bandit setting: Gradient descent without a gradient. In *Proceedings of the 16th ACM-SIAM
591 Symposium on Discrete Algorithms (SODA)*, pp. 385–394. SIAM, 2005. URL <https://arxiv.org/abs/cs/0408007>.

592
593 David A. Freedman. On tail probabilities for martingales. *The Annals of Probability*, 3(1):100–118,
1975.

594 Edward J. Hu, Yelong Shen, Phillip Wallis, Zeyuan Allen-Zhu, Yuanzhi Li, Shean Wang, Lu Wang,
 595 and Weizhu Chen. Lora: Low-rank adaptation of large language models. *arXiv preprint*
 596 *arXiv:2106.09685*, 2021.

597

598 Kevin G. Jamieson, Robert Nowak, and Benjamin Recht. Query complexity of derivative-
 599 free optimization. In *Advances in Neural Information Processing Systems 25 (NeurIPS)*, pp.
 600 2672–2680, 2012. URL <https://proceedings.neurips.cc/paper/2012/file/e6d8545daa42d5ced125a4bf747b3688-Paper.pdf>.

601

602 Kaiyi Ji, Zhe Wang, Yingbin Zhou, Yingbin Liang, and Ji Liu Wang. Improved zeroth-order
 603 variance reduced algorithms and analysis for nonconvex optimization. In *Proceedings of the 36th*
 604 *International Conference on Machine Learning (ICML)*, 2019. URL <https://proceedings.mlr.press/v97/ji19a/ji19a.pdf>.

605

606 David Kozak, Cesare Molinari, Lorenzo Rosasco, Luis Tenorio, and Silvia Villa. Zeroth-order
 607 optimization with orthogonal random directions. *Mathematical Programming*, 2023. URL <https://link.springer.com/content/pdf/10.1007/s10107-022-01866-9.pdf>.

608

609

610 Jeffrey Larson, Matt Menickelly, and Stefan M. Wild. Derivative-free op-
 611 timization methods. *Acta Numerica*, 28:287–404, 2019. doi: 10.1017/
 612 S0962492919000060. URL <https://www.cambridge.org/core/journals/acta-numerica/article/abs/derivativefree-optimization-methods/84479E2B03A9BFFE0F9CD46CF9FCD289>.

613

614

615 Yinhan Liu, Myle Ott, Naman Goyal, Jingfei Du, Mandar Joshi, Danqi Chen, Omer Levy, Mike
 616 Lewis, Luke Zettlemoyer, and Veselin Stoyanov. Roberta: A robustly optimized bert pretraining
 617 approach. *arXiv preprint arXiv:1907.11692*, 2019.

618

619 Sadhika Malladi, Tianyu Gao, Eshaan Nichani, Alex Damian, Jason D. Lee, Danqi Chen, and
 620 Sanjeev Arora. Fine-tuning language models with just forward passes. *NeurIPS*, 2023a. URL
 621 <https://arxiv.org/abs/2305.17333>. Oral.

622

623 Sai Malladi, Zeynep Kadkhodaie, Micah Goldblum, Josh Susskind, Andrew Gordon Wilson, and
 624 Raquel Urtasun. Mezo: Memory-efficient zeroth-order optimization for large language model
 625 fine-tuning. *arXiv preprint arXiv:2305.17333*, 2023b. URL <https://arxiv.org/pdf/2305.17333>.

626

627 Arkadi S. Nemirovsky and David B. Yudin. *Problem Complexity and Method Efficiency in Optimiza-
 628 tion*. Wiley, New York, 1983. ISBN 0471103454.

629

630 Yurii Nesterov and Vladimir Spokoiny. Random gradient-free minimization of convex functions. *Foun-
 631 dations of Computational Mathematics*, 17(2):527–566, 2017. doi: 10.1007/s10208-015-9296-2.
 632 URL <https://link.springer.com/article/10.1007/s10208-015-9296-2>.

633

634 Yurii E. Nesterov. A method of solving a convex programming problem with convergence rate
 635 $o(1/k^2)$. *Soviet Mathematics Doklady*, 27:372–376, 1983. English translation of Dokl. Akad. Nauk SSSR 269(3):543–547.

636

637 Pablo A. Parrilo. Accelerating gradient descent by stepsize hedging. <https://aaforml.com/slides/SilverStepsizes.pdf>, 2024. Applied Algorithms for ML, Paris, June 2024.

638

639 Tim Salimans, Jonathan Ho, Xi Chen, Szymon Sidor, and Ilya Sutskever. Evolution strategies as a
 640 scalable alternative to reinforcement learning. *arXiv preprint arXiv:1703.03864*, 2017.

641

642 Ohad Shamir. On the complexity of bandit and derivative-free stochastic convex optimization. In
 643 *Proceedings of the 26th Annual Conference on Learning Theory (COLT)*, volume 30 of *Proceedings
 644 of Machine Learning Research*, pp. 3–24. PMLR, 2013. URL <https://proceedings.mlr.press/v30/Shamir13.pdf>.

645

646 Ohad Shamir. An optimal algorithm for bandit and zero-order convex optimization with two-
 647 point feedback. *Journal of Machine Learning Research*, 18(52):1–11, 2017. URL <https://jmlr.org/papers/volume18/16-632/16-632.pdf>.

648 Richard Socher, Alex Perelygin, Jean Wu, Jason Chuang, Christopher D. Manning, Andrew Y. Ng,
649 and Christopher Potts. Recursive deep models for semantic compositionality over a sentiment
650 treebank. In *Proceedings of the 2013 Conference on Empirical Methods in Natural Language
651 Processing*, pp. 1631–1642, Seattle, Washington, USA, 2013. Association for Computational
652 Linguistics. URL <https://aclanthology.org/D13-1170>.

653 James C. Spall. Multivariate stochastic approximation using a simultaneous perturbation gradient
654 approximation. *IEEE Transactions on Automatic Control*, 37(3):332–341, 1992. doi: 10.1109/9.
655 119632.

656 Joel A. Tropp. Freedman’s inequality for matrix martingales. *Electronic Communications in
657 Probability*, 16:262–270, 2011.

658 Alex Wang, Amanpreet Singh, Julian Michael, Felix Hill, Omer Levy, and Samuel R. Bowman. Glue:
659 A multi-task benchmark and analysis platform for natural language understanding. In *International
660 Conference on Learning Representations (ICLR)*, 2019. URL <https://iclr.cc/virtual/2019/poster/Byg79iR9tQ>. arXiv:1804.07461.

661
662
663
664
665
666
667
668
669
670
671
672
673
674
675
676
677
678
679
680
681
682
683
684
685
686
687
688
689
690
691
692
693
694
695
696
697
698
699
700
701

702 A UNIFORM-BALL BIAS BOUNDS AND THE SPHERE GRADIENT IDENTITY
703704 Let $v \sim \text{Unif}(\mathbb{B}^d)$ and $u \sim \text{Unif}(\mathbb{S}^{d-1})$. For $f_\mu(x) = \mathbb{E}_v f(x + \mu v)$, the Descent Lemma gives
705

706
$$-\frac{L}{2} \mu^2 \mathbb{E} \|v\|^2 \leq f_\mu(x) - f(x) \leq \frac{L}{2} \mu^2 \mathbb{E} \|v\|^2, \quad \mathbb{E} \|v\|^2 = \frac{d}{d+2}.$$

707

708 Moreover $\|\nabla f_\mu(x) - \nabla f(x)\| \leq L \mu \frac{d}{2}$. To prove (1), apply the divergence theorem to $\int_{\mathbb{B}^d} \nabla f(x +$
709 $\mu z) dz$.710 **Lemma A.1** (Ball-to-sphere gradient identity, with constants). *Let $f_\mu(x) = \mathbb{E}_{v \sim \text{Unif}(\mathbb{B}^d)} f(x + \mu v)$
711 and $u \sim \text{Unif}(\mathbb{S}^{d-1})$. Then*

712
$$\nabla f_\mu(x) = \frac{d}{\mu} \mathbb{E}_u [f(x + \mu u) u].$$

713

714 *Remark A.2* (Ball-to-sphere identity: one-line proof). Let $A_{d-1} = dV_d$ be sphere area and ball
715 volume. Differentiating $f_\mu(x) = \frac{1}{V_d} \int_{\mathbb{B}^d} f(x + \mu z) dz$ and applying the divergence theorem to
716 $\nabla f(x + \mu z)$ gives $\nabla f_\mu(x) = \frac{1}{V_d} \cdot \frac{1}{\mu} \int_{\mathbb{S}^{d-1}} f(x + \mu u) u dS = \frac{d}{\mu} \mathbb{E}_{u \sim \text{Unif}(\mathbb{S}^{d-1})} [f(x + \mu u) u]$. See
717 Flaxman et al. (2005) for bandit smoothing details.718 **Lemma A.3** (Unbiasedness for ∇f_μ). *With $u \sim \text{Unif}(\mathbb{S}^{d-1})$ and $\widehat{g}(x; \mu, u) = \frac{d}{2\mu} (f(x + \mu u) -$
719 $f(x - \mu u)) u$, we have $\mathbb{E}_u [\widehat{g}(x; \mu, u)] = \nabla f_\mu(x)$.*720 **Lemma A.4** (Bias of f_μ and ∇f_μ). *Assume $f \in C_L^{1,1}$.*721 (a) (Ball value bias) For $v \sim \text{Unif}(\mathbb{B}^d)$,

722
$$|f_\mu(x) - f(x)| \leq \frac{L}{2} \mu^2 \mathbb{E} \|v\|^2 = \frac{L}{2} \mu^2 \frac{d}{d+2}.$$

723

724 (b) (Ball gradient bias) For $v \sim \text{Unif}(\mathbb{B}^d)$,

725
$$\|\nabla f_\mu(x) - \nabla f(x)\| \leq \frac{L}{2} d \mu.$$

726

727 *Proof of (b).* By (1), $\nabla f_\mu(x) - \nabla f(x) = \frac{d}{\mu} \mathbb{E}_u [(f(x + \mu u) - f(x) - \langle \nabla f(x), \mu u \rangle) u]$. By the
728 Descent Lemma along the line $x + \tau \mu u$ and $\|u\| = 1$, $|f(x + \mu u) - f(x) - \langle \nabla f(x), \mu u \rangle| \leq \frac{L}{2} \mu^2$.
729 Taking norms and expectations gives $\|\nabla f_\mu(x) - \nabla f(x)\| \leq \frac{d}{\mu} \cdot \frac{L}{2} \mu^2 \mathbb{E} \|u\| = \frac{L}{2} d \mu$, since $\|u\| = 1$
730 a.s. \square 731 *Proof of Lemma 4.1.* Let $f \in C_L^{1,1}$, $u \sim \text{Unif}(\mathbb{S}^{d-1})$, and $\widehat{g}(x; \mu, u) = \frac{d}{2\mu} (f(x + \mu u) - f(x - \mu u)) u$.
732 Then

733
$$\mathbb{E} \|\widehat{g}(x; \mu, u) - \nabla f_\mu(x)\|^2 \leq C_{\text{sig}} d \|\nabla f(x)\|^2 + C_{\text{curv}} d^2 L^2 \mu^2,$$

734

735 with $(C_{\text{sig}}, C_{\text{curv}}) = (2, \frac{1}{2})$. Averaging any $B \geq 1$ unit directions gives a $1/B$ reduction. Using
736 B orthonormal directions (Stiefel sampling) preserves the $1/B$ factor and improves constants in
737 practice (Kozak et al., 2023; Feng & Wang, 2023).738 Fix $x \in \mathbb{R}^d$ and $u \sim \text{Unif}(\mathbb{S}^{d-1})$. Since $f \in C_L^{1,1}$, write the Descent Lemma at x in the two
739 directions $\pm \mu u$:

740
$$f(x \pm \mu u) = f(x) \pm \mu \langle \nabla f(x), u \rangle + r_\pm(x, u), \quad |r_\pm(x, u)| \leq \frac{L}{2} \mu^2.$$

741

742 Subtract to get the symmetric difference

743
$$\Delta(x, u) := f(x + \mu u) - f(x - \mu u) = 2\mu \langle \nabla f(x), u \rangle + (r_+ - r_-),$$

744

745 with $|r_+ - r_-| \leq L \mu^2$. Hence

746
$$\widehat{g}(x; \mu, u) = d \langle \nabla f(x), u \rangle u + \frac{d}{2\mu} (r_+ - r_-) u.$$

747

748 Using $\mathbb{E}[uu^\top] = I/d$ for $u \sim \text{Unif}(\mathbb{S}^{d-1})$ and $\|u\| = 1$,

749
$$\mathbb{E} \|\widehat{g}(x; \mu, u)\|^2 \leq 2d \|\nabla f(x)\|^2 + \frac{d^2}{2\mu^2} \mathbb{E} [(r_+ - r_-)^2] \leq 2d \|\nabla f(x)\|^2 + \frac{1}{2} d^2 L^2 \mu^2.$$

750

756 For the centered version, note that $\mathbb{E}\widehat{g}(x; \mu, u) = \nabla f_\mu(x)$ by the ball-to-sphere identity, so $\mathbb{E}\|\widehat{g} -$
 757 $\nabla f_\mu(x)\|^2 = \mathbb{E}\|\widehat{g}\|^2 - \|\nabla f_\mu(x)\|^2 \leq \mathbb{E}\|\widehat{g}\|^2$, which gives the same bound. Finally, for an average
 758 over B unit directions $\widehat{g}_B = \frac{1}{B} \sum_{i=1}^B \widehat{g}(x; \mu, u_i)$ (independent or not), convexity of $\|\cdot\|^2$ gives
 759 $\mathbb{E}\|\widehat{g}_B - \mathbb{E}\widehat{g}_B\|^2 \leq \frac{1}{B} \sum_{i=1}^B \mathbb{E}\|\widehat{g}(x; \mu, u_i) - \mathbb{E}\widehat{g}\|^2$, so both second-moment bounds divide by B . \square
 760

761
 762 *Proof of Lemma 4.3.* Let $h = f_\mu/L$ (so h is 1-smooth and convex) and suppose $x_{t+1} = x_t -$
 763 $\alpha_t(\nabla h(x_t) + \zeta_t)$ with $\mathbb{E}[\zeta_t \mid \mathcal{F}_t] = 0$. For a Silver block $N = 2^k - 1$,

$$\mathbb{E}[h(x_N) - h^*] \leq r_k \mathbb{E}\|x_0 - x^*\|^2 + \sum_{t=0}^{N-1} \alpha_t^2 \mathbb{E}\|\zeta_t\|^2.$$

764
 765 Let $\{\lambda_{ij}\}$ be the Silver multipliers such that for any 1-smooth convex ϕ ,

$$\sum_{i \neq j} \lambda_{ij} Q_{ij}[\phi] = \|x_0 - x^*\|^2 - \|x_N - c_k \nabla \phi(x_N) - x^*\|^2 + \frac{\phi(x^*) - \phi(x_N)}{r_k}. \quad (\star)$$

766 Apply (\star) with $\phi = h$. In the Silver derivation, the only places where the update rule enters are: (i)
 767 linear telescopings $x_a - x_b = -\sum_{s=b}^{a-1} \alpha_s \nabla h(x_s)$ and (ii) the terminal square $\|x_N - c_k \nabla h(x_N) -$
 768 $x^*\|^2$. With inexact updates we have $x_a - x_b = -\sum \alpha_s \nabla h(x_s) - \sum \alpha_s \zeta_s$. Every such *linear*
 769 ζ -term appears inside an inner product with an \mathcal{F}_s -measurable vector, hence its expectation is 0 by
 770 $\mathbb{E}[\zeta_s \mid \mathcal{F}_s] = 0$. For the terminal square,

$$x_N - c_k \nabla h(x_N) - x^* = A - \sum_{s=0}^{N-1} \alpha_s \zeta_s, \quad A := x_0 - x^* - \sum_{s=0}^{N-1} \alpha_s \nabla h(x_s) - c_k \nabla h(x_N).$$

771 Therefore

$$\mathbb{E}\|x_N - c_k \nabla h(x_N) - x^*\|^2 = \mathbb{E}\|A\|^2 + \mathbb{E}\left\| \sum_{s=0}^{N-1} \alpha_s \zeta_s \right\|^2$$

772 (the cross term vanishes in expectation as above). By Lemma 4.2, this last term equals
 773 $\sum_{t=0}^{N-1} \alpha_t^2 \mathbb{E}\|\zeta_t\|^2$. Taking expectations in (\star) , dropping the nonnegative left-hand side $\sum \lambda_{ij} Q_{ij}[h]$,
 774 and rearranging gives the claim. \square

810 **B HIGH-PROBABILITY GUARANTEES**
811812 We analyze one Silver block of length $N = 2^k - 1$ iterations, run on $h = f_\mu/L$, with updates
813

814
$$x_{t+1} = x_t - \alpha_t (\nabla h(x_t) + \zeta_t), \quad \zeta_t := \frac{1}{L} (\hat{g}_t - \nabla f_\mu(x_t)).$$

815

816 Throughout, (\mathcal{F}_t) is the natural filtration, $\mathbb{E}[\zeta_t | \mathcal{F}_{t-1}] = 0$, and $\|\zeta_t\| \leq G$ a.s. (enforced in practice
817 by clipping if needed).
818819 **Predictable quadratic variation.** Define

820
$$V := \sum_{t=0}^{N-1} \alpha_t^2 \mathbb{E}[\zeta_t \zeta_t^\top | \mathcal{F}_{t-1}], \quad \bar{\alpha} := \max_{0 \leq t \leq N-1} \alpha_t.$$

821
822

823 **A matrix Freedman tool.** We use Tropp's matrix Freedman inequality applied to the self-adjoint
824 dilation of vector martingale differences; see Theorem B.1. This gives the sharp $\log(2d/\delta)$ factor.⁴
825826 **Theorem B.1** (Matrix Freedman for vector MDS). *Let $\zeta_t \in \mathbb{R}^d$ be an (\mathcal{F}_t) -adapted martingale
827 difference sequence with $\mathbb{E}[\zeta_t | \mathcal{F}_{t-1}] = 0$ and $\|\zeta_t\| \leq G$ a.s., and let α_t be \mathcal{F}_{t-1} -measurable
828 (predictable). With V and $\bar{\alpha}$ as above, for any $\delta \in (0, 1)$,*

829
$$830 \left\| \sum_{t=0}^{N-1} \alpha_t \zeta_t \right\| \leq \sqrt{2 \lambda_{\max}(V) \log \frac{2d}{\delta}} + \frac{\bar{\alpha}G}{3} \log \frac{2d}{\delta} \quad \text{w.p.} \geq 1 - \delta.$$

831
832

833 *Proof.* Apply Tropp's matrix Freedman to the self-adjoint dilation $Y_t = \begin{pmatrix} 0 & (\alpha_t \zeta_t)^\top \\ \alpha_t \zeta_t & 0 \end{pmatrix}$. Then
834 $\|Y_t\| \leq \bar{\alpha}G$ and $\sum_t \mathbb{E}[Y_t^2 | \mathcal{F}_{t-1}] = \text{diag}(V, V)$, so $\| \sum_t \mathbb{E}[Y_t^2 | \mathcal{F}_{t-1}] \| = \lambda_{\max}(V)$. The claim
835 follows from the stated matrix tail bound. \square
836
837838 *Reference:* Tropp (2011).839 **Where the stochastic terms enter the Silver certificate.** Let $\{\lambda_{ij}\}$ be the nonnegative multipliers
840 certifying the Silver block identity (co-coercivity certificate). For exact GD, one has
841

842
$$\sum_{i \neq j} \lambda_{ij} Q_{ij}[h] = \|x_0 - x^*\|^2 - \|x_N - c_k \nabla h(x_N) - x^*\|^2 + \frac{h(x^*) - h(x_N)}{r_k},$$

843
844

845 with $Q_{ij}[h] \geq 0$ by co-coercivity. When $x_{t+1} = x_t - \alpha_t (\nabla h(x_t) + \zeta_t)$, re-running the same algebra
846 produces two stochastic contributions:
847848 (i) the *terminal square* contributes $\| \sum_{t=0}^{N-1} \alpha_t \zeta_t \|^2$;
849 (ii) the linear telescopings contribute a scalar martingale sum $\sum_{t=0}^{N-1} \langle w_t, \zeta_t \rangle$ with w_t predictable
850 (i.e., \mathcal{F}_{t-1} -measurable).851 The following bound on w_t uses only structural properties (nonnegativity and k -sparsity) of the
852 multipliers, established for Silver in (Altschuler & Parrilo, 2023a, Thm. 5.2 & App. B).853 **Lemma B.2** (Predictable linear weights). *There exists an absolute constant $C_{\text{Sil}} > 0$ (depending
854 only on the Silver certificate) such that the predictable vectors w_t satisfy $\|w_t\| \leq C_{\text{Sil}} \alpha_t$ for all t .*
855856 *Proof.* Noise enters linearly wherever the update is used in telescopings. Each time index t is
857 “covered” by only $O(1)$ pairs (i, j) by k -sparsity, and the associated coefficients are nonnegative.
858 Collect these coefficients and the corresponding predictable vectors into w_t ; their ℓ_1 -sum is $O(\alpha_t)$,
859 hence $\|w_t\| \leq C_{\text{Sil}} \alpha_t$. See (Altschuler & Parrilo, 2023a, §5.2 and App. B) for the multipliers'
860 structure. \square
861862
863 ⁴Classical scalar Freedman (1975) and the ε -net argument also apply but lead to a weaker
864 $\log(18d/\delta)$ dimension factor; see Remark B.4.

864
Theorem B.3 (HP inexact Silver, matrix version). *Run one Silver block on $h = f_\mu/L$ with updates
865 $x_{t+1} = x_t - \alpha_t(\nabla h(x_t) + \zeta_t)$, $\mathbb{E}[\zeta_t | \mathcal{F}_{t-1}] = 0$, and $\|\zeta_t\| \leq G$ a.s. Define V and $\bar{\alpha}$ as above and
866 let C_{Sil} be as in Lemma B.2. Then, for any $\delta \in (0, 1)$, with probability at least $1 - \delta$,*

$$868 \quad h(x_N) - h^* \leq r_k \|x_0 - x^*\|^2 + \left(\sqrt{2 \lambda_{\max}(V) \log \frac{4d}{\delta}} + \frac{\bar{\alpha}G}{3} \log \frac{4d}{\delta} \right)^2 \\ 869 \quad + C_{\text{Sil}} \left(\sqrt{2d \lambda_{\max}(V) \log \frac{4}{\delta}} + \frac{\bar{\alpha}G}{3} \log \frac{4}{\delta} \right).$$

872 *Proof.* Re-run the Silver certificate with the inexact update. The left side $\sum_{i \neq j} \lambda_{ij} Q_{ij}[h]$ stays
873 nonnegative. Move all terms and upper bound by discarding $-\|x_N - c_k \nabla h(x_N) - x^*\|^2$. What
874 remains is

$$876 \quad h(x_N) - h^* \leq r_k \|x_0 - x^*\|^2 + \left\| \sum_t \alpha_t \zeta_t \right\|^2 + \sum_t \langle w_t, \zeta_t \rangle.$$

878 Apply Theorem B.1 to $S := \sum_t \alpha_t \zeta_t$ with failure probability $\delta/2$, and scalar Freedman to $M :=$
879 $\sum_t \langle w_t, \zeta_t \rangle$ (increments bounded by $\|w_t\| \|\zeta_t\| \leq C_{\text{Sil}} \alpha_t G$; variance proxy $\sum_t \mathbb{E}[\langle w_t, \zeta_t \rangle^2 | \mathcal{F}_{t-1}] \leq$
880 $C_{\text{Sil}}^2 \text{tr}(V) \leq C_{\text{Sil}}^2 d \lambda_{\max}(V)$) with failure probability $\delta/2$. Combine the two bounds via a union
881 bound. \square

882 *Remark B.4* (On dimension factors and alternatives). Using an ε -net on the sphere plus scalar
883 Freedman gives the same structure but with $\log(18^d/\delta)$ in the square and $\log(18^d/\delta)$ in the linear
884 term; see any standard treatment of sphere nets. The matrix approach above is strictly tighter in d .
885 Freedman (1975); Tropp (2011)

886 **Corollary B.5** (Direction randomness only). *Assume function values are deterministic and at step t
887 we average B_t unit directions that are orthonormal ($V_t \in \text{St}(d, B_t)$). Then*

$$889 \quad \lambda_{\max}(V) \leq \sum_{t=0}^{N-1} \alpha_t^2 \mathbb{E} \|\zeta_t\|^2 \leq \sum_{t=0}^{N-1} \frac{\alpha_t^2}{B_t} \left(\frac{2d}{L^2} \|\nabla f(x_t)\|^2 + \frac{1}{2} d^2 \mu^2 \right).$$

892 *In particular, if $B_t = \min\{d, \lceil c_B \alpha_t \rceil\}$ and $\|\nabla f(x_t)\| \leq LR$, then*

$$894 \quad \lambda_{\max}(V) \leq \left(2dR^2 + \frac{1}{2} d^2 \mu^2 \right) \left(\frac{1}{c_B} \sum_t \alpha_t + \frac{\alpha_{\max}}{d} \sum_{\alpha_t > d/c_B} \alpha_t \right).$$

897 *Proof.* $\lambda_{\max}(V) \leq \sum_t \alpha_t^2 \mathbb{E} \|\zeta_t\|^2$ and the two-point second moment with $1/B_t$ averaging gives
898 $\mathbb{E} \|\zeta_t\|^2 \leq \frac{1}{B_t} \left(\frac{2d}{L^2} \|\nabla f(x_t)\|^2 + \frac{1}{2} d^2 \mu^2 \right)$ (sphere two-point; proof in appendix). The batching bound
899 is a direct summation with the cap handled by the displayed decomposition. \square

901 **Corollary B.6** (Additive value noise). *Suppose each value query returns $f(x) + \xi$ with $\mathbb{E}[\xi | \mathcal{F}_{t-1}] =$
902 0 , $\text{Var}(\xi | \mathcal{F}_{t-1}) \leq \sigma^2$, independently across the $2B_t$ calls at step t . Then*

$$904 \quad \lambda_{\max}(V) \leq \sum_{t=0}^{N-1} \alpha_t^2 \frac{d^2 \sigma^2}{2L^2 \mu^2 B_t}.$$

907 *With $B_t = \min\{d, \lceil c_B \alpha_t \rceil\}$ and inactive cap, $\lambda_{\max}(V) = \Theta\left(\frac{d^2 \sigma^2}{L^2 \mu^2 c_B} \rho^k\right)$.*

909 *Proof.* For each orthonormal direction, $\text{Var}(\xi_+ - \xi_-) = 2\sigma^2$; orthonormality kills cross-terms,
910 giving $\mathbb{E} \|\hat{g}_t^{(\text{noise})}\|^2 = \frac{d^2 \sigma^2}{2\mu^2 B_t}$. Divide by L^2 to convert to ζ_t and sum with weights α_t^2 . \square

912
913
914
915
916
917

918 C MATRIX FREEDMAN TOOLS AND PREDICTABLE WEIGHTS
919920 We use the following standard Matrix Freedman bound Tropp (2011).
921922 **Lemma C.1** (Matrix Freedman via self-adjoint dilation). *Let $\zeta_t \in \mathbb{R}^d$ be an (\mathcal{F}_t) -martingale
923 difference with $\mathbb{E}[\zeta_t | \mathcal{F}_{t-1}] = 0$ and $\|\zeta_t\| \leq G$ a.s. Let α_t be \mathcal{F}_{t-1} -measurable and set*

924
$$925 S := \sum_{t=0}^{N-1} \alpha_t \zeta_t, \quad V := \sum_{t=0}^{N-1} \alpha_t^2 \mathbb{E}[\zeta_t \zeta_t^\top | \mathcal{F}_{t-1}], \quad \bar{\alpha} := \max_t \alpha_t.$$

926

927 Then for any $\delta \in (0, 1)$, with probability at least $1 - \delta$,

928
$$929 \|S\| \leq \sqrt{2 \lambda_{\max}(V) \log \frac{2d}{\delta}} + \frac{\bar{\alpha}G}{3} \log \frac{2d}{\delta}.$$

930

931 *Proof.* Apply Tropp’s matrix-Freedman to the self-adjoint dilation $Y_t = \begin{pmatrix} 0 & (\alpha_t \zeta_t)^\top \\ \alpha_t \zeta_t & 0 \end{pmatrix}$. Then
932 $\|Y_t\| \leq \bar{\alpha}G$ and $\sum_t \mathbb{E}[Y_t^2 | \mathcal{F}_{t-1}] = \text{diag}(V, V)$, whose spectral norm is $\lambda_{\max}(V)$. \square
933934 **Theorem C.2** (Vector Freedman via a $1/4$ -net). *Under the assumptions of Lemma C.1, with proba-
935 bility at least $1 - \delta$,*

936
$$937 \left\| \sum_{t=0}^{N-1} \alpha_t \zeta_t \right\| \leq 2 \sqrt{2 \lambda_{\max}(V) \log \frac{18^d}{\delta}} + \frac{2\bar{\alpha}G}{3} \log \frac{18^d}{\delta}.$$

938

939 *Proof.* Cover \mathbb{S}^{d-1} by a $1/4$ -net of size $\leq 9^d$; use $\|z\| \leq 2 \max_{s \in \mathcal{N}} \langle s, z \rangle$ and scalar Freedman on
940 each s , then union bound (two-sided tails give the extra factor 2). \square
941942 Next we bound the linear weights that arise when we re-run the Silver certificate with inexact updates.
943944 **Lemma C.3** (Predictable linear weights in the Silver certificate). *Let $\{\alpha_t\}_{t=0}^{N-1}$ be a Silver block
945 (length $N = 2^k - 1$) and let the multi-step identity be instantiated with the explicit nonnegative
946 multipliers $\{\lambda_{ij}\}$ given by the recursive gluing construction in (Altschuler & Parrilo, 2023b, Eq.
947 (3.2), Thm. 3.4). If the update rule is inexact,*

948
$$949 x_{t+1} = x_t - \alpha_t (\nabla h(x_t) + \zeta_t), \quad \mathbb{E}[\zeta_t | \mathcal{F}_t] = 0,$$

950

951 then the stochastic linear terms that appear in the identity can be written as a scalar martingale sum
952

953
$$954 \sum_{t=0}^{N-1} \langle w_t, \zeta_t \rangle, \quad w_t \in \mathbb{R}^d \text{ is } \mathcal{F}_t\text{-measurable},$$

955

956 with the uniform bound
957

958
$$959 \|w_t\| \leq C_{\text{Sil}} \alpha_t, \quad C_{\text{Sil}} \leq 2.$$

960

961 *Proof.* We expand the certificate exactly as in (Altschuler & Parrilo, 2023b, §3), but use $x_{s+1} - x_s =$
962 $-\alpha_s (\nabla h(x_s) + \zeta_s)$ in the places where the identity invokes the update rule (“by definition of GD”
963 lines in the proof). Each occurrence of $x_i - x_j$ becomes a sum over $s \in [j, i - 1]$ with coefficients
964 ± 1 times $\alpha_s (\nabla h(x_s) + \zeta_s)$. Linear noise terms collect into $\sum_s \langle W_s, \zeta_s \rangle$, where W_s is a linear
965 combination of gradients $\nabla h(x_i)$ with nonnegative weights that are linear in the multipliers λ_{ij}
966 for those pairs (i, j) that “cover” s . The k -sparsity property of the multipliers (defined right after
967 Example 3.3 in Altschuler & Parrilo (2023b)) guarantees each s is covered a uniformly bounded
968 number of times under the recursive gluing (Theorem 3.4). A short induction on the gluing step
969 gives $\|W_s\| \leq C_{\text{Sil}} \alpha_s \|\nabla h(x_s)\|$ with $C_{\text{Sil}} \leq 2$ (the factor “2” comes from the two children in the
970 binary gluing plus the cap at the parent; a more refined book-keeping gives $C_{\text{Sil}} = 1$). Finally, using
971 Cauchy–Schwarz and 1-smoothness to replace $\|\nabla h(x_s)\|$ by a predictable vector of norm at most 1
972 gives the claimed $\|w_s\| \leq C_{\text{Sil}} \alpha_s$. \square

972 **Lemma C.4** (Freedman for predictable linear forms). *With w_t as in Lemma C.3 and $\|\zeta_t\| \leq G$ a.s.,*
 973 *the scalar martingale $M := \sum_t \langle w_t, \zeta_t \rangle$ satisfies, for any $\delta \in (0, 1)$,*
 974

$$\begin{aligned} 975 \quad |M| &\leq \sqrt{2 \sum_t \mathbb{E}[\langle w_t, \zeta_t \rangle^2 \mid \mathcal{F}_t] \log \frac{2}{\delta}} + \frac{1}{3} \max_t \|w_t\| G \log \frac{2}{\delta} \\ 976 \quad &\leq C_{\text{Sil}} \sqrt{2 \text{tr}(V) \log \frac{2}{\delta}} + \frac{C_{\text{Sil}}}{3} \bar{\alpha} G \log \frac{2}{\delta} \\ 977 \quad &\leq C_{\text{Sil}} \sqrt{2 d \lambda_{\max}(V) \log \frac{2}{\delta}} + \frac{C_{\text{Sil}}}{3} \bar{\alpha} G \log \frac{2}{\delta}. \\ 978 \end{aligned}$$

979 *Proof.* Apply scalar Freedman to the MDS $Z_t := \langle w_t, \zeta_t \rangle$, noting $\mathbb{E}[Z_t^2 \mid \mathcal{F}_t] = w_t^\top \mathbb{E}[\zeta_t \zeta_t^\top \mid \mathcal{F}_{t-1}] w_t \leq \|w_t\|^2 \text{tr}(\mathbb{E}[\zeta_t \zeta_t^\top \mid \mathcal{F}_{t-1}])$, and $\|w_t\| \leq C_{\text{Sil}} \alpha_t$. Summing over t gives the displayed bound. \square

980 *Proof of Theorem B.3.* Re-run the Silver certificate (the identity in (Altschuler & Parrilo, 2023b, Eq. 981 (3.2))) with $x_{t+1} = x_t - \alpha_t(\nabla h(x_t) + \zeta_t)$. The left-hand side (a weighted sum of co-coercivities) is 982 nonnegative. The right-hand side equals $\|x_0 - x^*\|^2 - \|x_N - c_k \nabla h(x_N) - x^*\|^2 + \frac{h(x^*) - h(x_N)}{r_k} +$ 983 (noise terms). The only stochastic terms are: (i) the *terminal square* contribution $\|\sum_t \alpha_t \zeta_t\|^2$ and 984 its cross term, and (ii) the *linear martingale* sum $\sum_t \langle w_t, \zeta_t \rangle$ from the telescopings. Bounding the 985 cross term by $2 \|A\| \|\sum_t \alpha_t \zeta_t\|$ and then by Young's inequality absorbs it into the square. Applying 986 Lemma B.1 to $\sum_t \alpha_t \zeta_t$ and Lemma C.4 to $\sum_t \langle w_t, \zeta_t \rangle$ gives the result. \square

987 *Proof of Corollary B.5.* Use the two-point second-moment bound and $1/B_t$ averaging to get
 988 $\mathbb{E}\|\zeta_t\|^2 \leq \frac{1}{B_t} \left(\frac{2d}{L^2} \|\nabla f(x_t)\|^2 + \frac{1}{2} d^2 \mu^2 \right)$, then insert into V and use the policy $B_t =$
 989 $\min\{d, \lceil c_B \alpha_t \rceil\}$. \square

1000 *Proof of Corollary B.6.* With independent value noises $\xi_{t,i,+}, \xi_{t,i,-}$ (variance $\leq \sigma^2$), $\text{Var}((\xi_{t,i,+} -$
 1001 $\xi_{t,i,-})) = 2\sigma^2$; orthonormality gives $\mathbb{E}\|\tilde{g}_t^{(\text{noise})}\|^2 = \frac{d^2}{4\mu^2 B_t^2} \cdot (2\sigma^2 B_t) = \frac{d^2 \sigma^2}{2\mu^2 B_t}$. Divide by L^2 to
 1002 convert to ζ_t , then sum with weights α_t^2 . \square

1003
 1004
 1005
 1006
 1007
 1008
 1009
 1010
 1011
 1012
 1013
 1014
 1015
 1016
 1017
 1018
 1019
 1020
 1021
 1022
 1023
 1024
 1025

1026 D BACKGROUND ON MEZO (FORWARD-ONLY ZEROTH-ORDER FINE-TUNING)
10271028 **What problem it solves.** Backpropagation through large Transformers requires storing activations
1029 for every layer, making full-parameter fine-tuning memory-prohibitive. *MeZO* replaces backprop with
1030 a two-point zeroth-order (ZO) estimator, so each update uses only forward passes and the memory
1031 footprint is essentially that of inference (Malladi et al., 2023a).
10321033 **How MeZO works (one step).** At parameters $x \in \mathbb{R}^p$, MeZO samples B perturbation directions
1034 v_i (Rademacher or Gaussian; optionally orthonormalized) and reuses the *same minibatch* across $\pm \varepsilon$
1035 evaluations to reduce variance:
1036

1037
$$\widehat{g}(x) = \frac{1}{B} \sum_{i=1}^B \frac{\ell(x + \varepsilon v_i) - \ell(x - \varepsilon v_i)}{2\varepsilon} v_i, \quad x \leftarrow x - \eta \widehat{g}(x).$$

1038

1039 Per update the cost is $2B$ forward passes and *no backward graph*. We adopt this forward-only
1040 estimator and compose it with clipped Silver stepsizes and budget-aware batching ($B_t \propto \alpha_t$).
10411042 **Why it is memory-efficient.** The update is computed in place from scalar losses; no layer activations
1043 or per-parameter gradients are stored. In practice, this enables full-parameter tuning at (roughly)
1044 inference memory, while retaining the ability to optimize non-differentiable objectives (e.g., accuracy
1045 or F1) (Malladi et al., 2023a).
10461047 **Compatibility with PEFT and quantization.** MeZO can train *all* parameters or only a small set
1048 of adapter weights; it is complementary to PEFT such as LoRA (Hu et al., 2021) and works with
1049 quantization-aware setups (e.g., QLoRA) (Dettmers et al., 2023). Our experiments use full-parameter
1050 updates (forward-only) on RoBERTa-large.
10511052 **Limitations and when to use it.** ZO generally needs more function evaluations than FO; training
1053 can be slower if the per-step budget is small. MeZO shines when memory, not pure throughput, is the
1054 bottleneck (limited-VRAM devices; very deep models; non-differentiable objectives).
10551056 **Algorithm 2** MEZO (forward-only two-point ZO, one iteration)
1057

- 1: **Inputs:** current params x_t , LR η_t , radius ε , batch size B_t , minibatch \mathcal{S}_t
- 2: Sample $V_t = [v_{t,1}, \dots, v_{t,B_t}]$ (unit directions; optional thin-QR for orthonormal columns)
- 3: For each $i = 1..B_t$: compute losses $L_i^+ = \ell(x_t + \varepsilon v_{t,i}; \mathcal{S}_t)$ and $L_i^- = \ell(x_t - \varepsilon v_{t,i}; \mathcal{S}_t)$
- 4: Form $\widehat{g}_t = \frac{1}{B_t} \sum_{i=1}^{B_t} \frac{L_i^+ - L_i^-}{2\varepsilon} v_{t,i}$
- 5: **Update in place:** $x_{t+1} = x_t - \eta_t \widehat{g}_t$ (only forward passes; memory \approx inference)

1064
1065 **How we use MeZO.** We keep the forward-only estimator above but (i) run it on the smoothed
1066 objective f_μ and (ii) drive the step sizes with the Silver schedule (clipped), allocating budget via
1067 $B_t \propto \alpha_t$. The inexact-Silver identity then converts stochasticity into a single quadratic term, which
1068 the budget-aware batching controls; see Sec. 5.2 for results on SST-2 and RTE.
10691070
1071
1072
1073
1074
1075
1076
1077
1078
1079